Evaluation of uncertainties originating from the different modeling approaches applied to analyze regional groundwater flow in the Tono area of Japan

Yuji Ijiri [a,*], Hiromitsu Saegusa [b], Atsushi Sawada [c], Makoto Ono [a], Kunio Watanabe [d], Kenzi Karasaki [e], Christine Doughty [e], Michito Shimo [f], Kenichi Fumimura [f]

[a] *Taisei Corporation, Nuclear Facilities Division, 1-25-1 Nishi Shinjyuku, Shinjyuku-ku, Tokyo 163-0606, Japan*
[b] *Japan Atomic Energy Agency, Tono Geoscience Center, 1-64 Yamanouchi, Akiyo-cho, Mizunami-shi, Gifu 509-6132, Japan*
[c] *Japan Atomic Energy Agency, Geological Isolation Research and Development Directorate, 4-33 Tokai-mura, Nakagun, Ibaraki 319-1194, Japan*
[d] *Saitama University, 255 Shimo-Okubo, Saitama 338-8570, Japan*
[e] *Lawrence Berkeley National Laboratory, Earth Science Division, One Cyclotron Road, MS: 90-1116, Berkeley, California 94720, USA*
[f] *Taisei Corporation, Technology Research Center, 344-1 Nasemachi, Totsuka-ku, Yokohama 245-0051, Japan*

ARTICLE INFO

Article history:
Received 3 March 2008
Received in revised form 15 October 2008
Accepted 17 October 2008
Available online xxxx

Keywords:
Modeling
Uncertainty
Heterogeneity

ABSTRACT

Qualitative evaluation of the effects of uncertainties originating from scenario development, modeling approaches, and parameter values is an important subject in the area of safety assessment for high-level nuclear waste disposal sites. In this study, regional-scale groundwater flow analyses for the Tono area, Japan were conducted using three continuous models designed to handle heterogeneous porous media. We evaluated the simulation results to quantitatively analyze uncertainties originating from modeling approaches. We found that porous media heterogeneity is the main factor which causes uncertainties. We also found that uncertainties originating from modeling approaches greatly depend on the types of hydrological structures and heterogeneity of hydraulic conductivity values in the domain assigned by modelers. Uncertainties originating from modeling approaches decrease as the amount of labor and time spent increase, and iterations between investigation and analyses increases.

1. Introduction

Qualitative evaluation of the effects of uncertainties originating from scenario development, modeling approaches, and parameter values is an important subject in the area of safety assessment of high-level nuclear waste disposal (Nuclear Energy Agency, 1991). In order to evaluate uncertainties in scenario development, we create an FEP list containing presumable features (F), events (E) and processes (P) for safety assessment as the first step. We generate scenarios based on this list and evaluate each scenario (Japan Nuclear Cycle Development Institute, 1999). Many studies have been conducted to evaluate parameter uncertainties. These studies include reliability analysis of parameter values obtained from laboratory and in-situ experiments (Ijiri et al., 2004) and stochastic evaluation of parameter uncertainties on safety assessment (Wakasugi et al., 2000).

Few studies which focused on the evaluation of uncertainties in conceptual models of in-situ settings have been conducted. Zimmerman et al. (1998) compared seven geostatistically based inverse approaches to estimate transmissivities for modeling advective transport by groundwater flow. They conducted simulations of non-reactive tracer tests in a hypothetical domain which included hydraulic conductivities and head values from the Waste Isolation Pilot Plant site, U.S.A.,

* Corresponding author. Tel.: +81 3 5381 5315; fax: +81 3 3345 8330.
E-mail addresses: ijiri@ce.taisei.co.jp (Y. Ijiri), saegusa.hiromitsu@jaea.go.jp (H. Saegusa), sawada.atsushi@jaea.go.jp (A. Sawada), kunio@post.saitama-u.ac.jp (K. Watanabe), kkarasaki@lbl.gov (K. Karasaki), michito.shimo@sakura.taisei.co.jp (M. Shimo).

and calculated tracer pathways and travel times. They concluded that the magnitude of model uncertainties depended not only on assumptions, numerical discretization, and limitations in each model but also on the skills and experiences of modelers and amount of labor and time spent to the develop models.

Selroos et al. (2002) conducted simulations of flow and transport in fractured rock at the Äspö island, Sweden using continuous, fracture network, and channel network models and compared travel lengths, travel times, and discharge amounts. They found that the boundary conditions and dominant fractures greatly affected groundwater flow and transport and uncertainties arose due to characteristics of each numerical model.

Based on the results of these studies mentioned above we can summarize that three main factors, which are described in Fig. 1, cause uncertainties. These factors are: (1) caliber of modelers, i.e., skills and experiences of modelers, and labor and time spent to develop models, (2) simulation domain setup, i.e., the location and physical properties of hydrogeological systems which are interpreted from in-situ data, and boundary conditions for numerical analysis, and (3) conceptual models including modeling approaches used to describe geological media and numerical models. In order to handle uncertainties associated with conceptual models, modelers tend to assume several alternative models for a site and use various criteria in order to (1) rank these models, (2) eliminate some of them, and/or (3) weigh and average predictions and statistics generated by multiple models (e.g., Ye et al., 2008a,b; Refsgaarda et al., 2006) This leads issues related to model selection criteria and the issues receive greater attentions in recent years (Foglia et al., 2007; Ye et al., 2008a,b).

We have been investigating uncertainty associated with modeling approaches for groundwater flow field evaluation (Ijiri et al., 2007). The investigation involved model development and analysis of groundwater flow fields based on three conceptual models for the groundwater flow system in the Tono area, Japan. In order to evaluate uncertainties in regional groundwater flow systems of the Tono area, we focused on all three factors except the conceptual models factor (Fig. 1). In the study, we chose three modeling teams that developed three different codes based on different modeling approaches. We found that uncertainties originating from differences between interpretations among modelers, such as assigning different numerical domain geometry and size, boundary conditions, and modeling structures have a great impact on the results of regional groundwater flow as noted by aforementioned literatures.

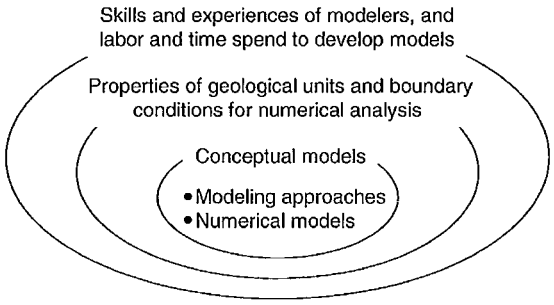

Fig. 1. Sources of uncertainties in groundwater flow analysis.

In this paper, we focus on modeling approaches including modeling structures of factor (2) and modeling heterogeneity of porous media of factor (3) described in Fig. 1. The modeling approaches chosen are all based on continuum porous media equivalency because more complex discrete representation of geological media require longer computational times. The modeling approaches are represented in three different codes TOUGH2, EQUIV_FLO, and Don-Chan. In TOUGH2, a probabilistic approach is adapted for modeling a heterogeneous hydraulic conductivity field based on the hydraulic conductivity distribution obtained from the in-situ hydraulic tests. EQUIV_FLO generated an equivalent heterogeneous hydraulic conductivity field by calculating a hydraulic conductivity tensor from the discrete fracture network constructed by using fracture characteristics obtained from the in-situ measurement. Don-Chan used a deterministic approach where a homogeneous hydraulic conductivity is assigned for each hydrogeological structure including faults as well as geological units. An equivalent pipe network is constructed for the complex structure of continuum rock formations and discontinuous faults.

We do not examine uncertainty originating from "numerical models" (one component in (3) in Fig. 1) in this study. This is because many studies have been conducted to evaluate numerical errors associated with uncertainties caused by numerical discretization methods, such as finite element and finite different methods, and the shape and size of discretized element. In addition, uncertainty originating from numerical models has been considered to be much less significant when compared to other factors.

2. Background of the Tono area

2.1. Topography and geological structures

The Tono area is characterized as a terrain that forms a bowl shape with a NE–SW axis, surrounded by the Mino–Hida mountain district in the northwest and the Mikawa mountain district in the southeast. The Kiso River flows in the north of the terrain and the Toki River flows from northeast to southwest in the central region. The study area that is used for the large-scale groundwater flow analysis, which will be mentioned later, is characterized as a terrain bounded by the Kiso River and the Toki River. The area gently slopes from northeast to southwest at a maximum slope of 4% at an altitude 150–400 m (see Fig. 2).

As shown in Fig. 3, the Neogene sedimentary rock unconformably overlies the Mesozoic basement rock. The Mesozoic basement rock consists of sedimentary rocks that belong to the Mino Belt, the Nohi rhyolite that overlies the sedimentary rocks and the Late Cretaceous Toki granite that intrudes above both rock types. The Toki granite occupies most of the basement rock area in the domain and consists mainly of fine- to coarse-grained biotite granite.

The Neogene sedimentary rock consists of the Miocene Mizunami Group and Pliocene Seto Group. The Seto Group unconformably overlies the Mizunami Group. The Mizunami Group consists of marine sedimentary rocks derived from transgression. The Mizunami Group slopes toward the south and is divided into 4 formations. The Toki lignite-bearing formation consists of lignite-bearing mudstone and sandstone and unconformably overlies basement rock with a

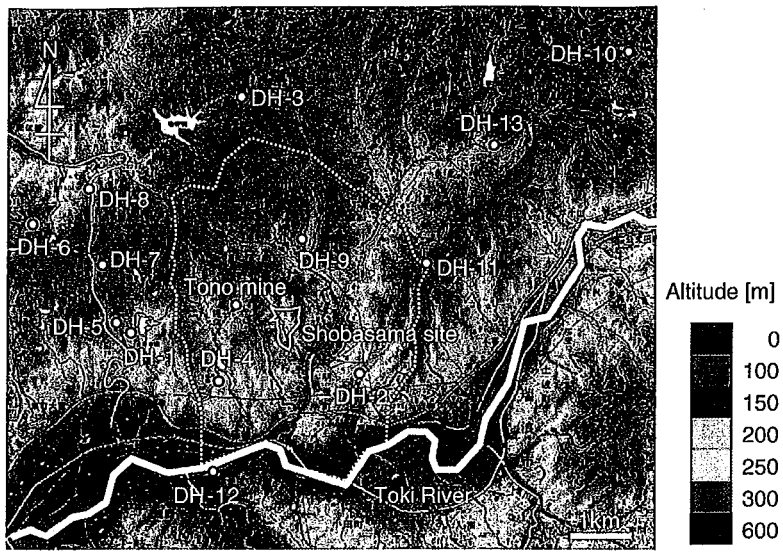

Fig. 2. Topographic map of the Tono region and borehole locations.

conglomerate layer. The Hongo formation is composed of tuffaceous sandstone–siltstone–mudstone alternations along with conglomerate. The Akeyo formation is composed of tuffaceous sandstone–mudstone that has a thin layer of tuff in the middle. The Oidawara formation consists of unstratified siltstone, fine tuffaceous mudstone, and conglomerate with medium-coarse sandstone in the basal horizon. The Seto Group is horizontally distributed throughout the study area and consists of clay and gravelly sand.

The Tsukiyoshi fault extends through the center of the assessment area having an E–W strike. According to the results of borehole investigations the Tsukiyoshi fault has a N80°W strike, 70°S dip, 10–30 m width, and approximately 30 m vertical displacement. From the result of stratigraphic studies it is assumed that the Tsukiyoshi fault was active during the periods between the deposition of the Oidawara formation and the Seto Group. In addition, the Tsukiyoshi fault is considered to have a low permeability zone near the center because pore water pressure is approximately 30 m higher in the foot wall than the hanging wall.

2.2. Data obtained from site investigation

Various types of investigations have been conducted in order to evaluate large-scale groundwater flow system in the Tono area (Table 1).

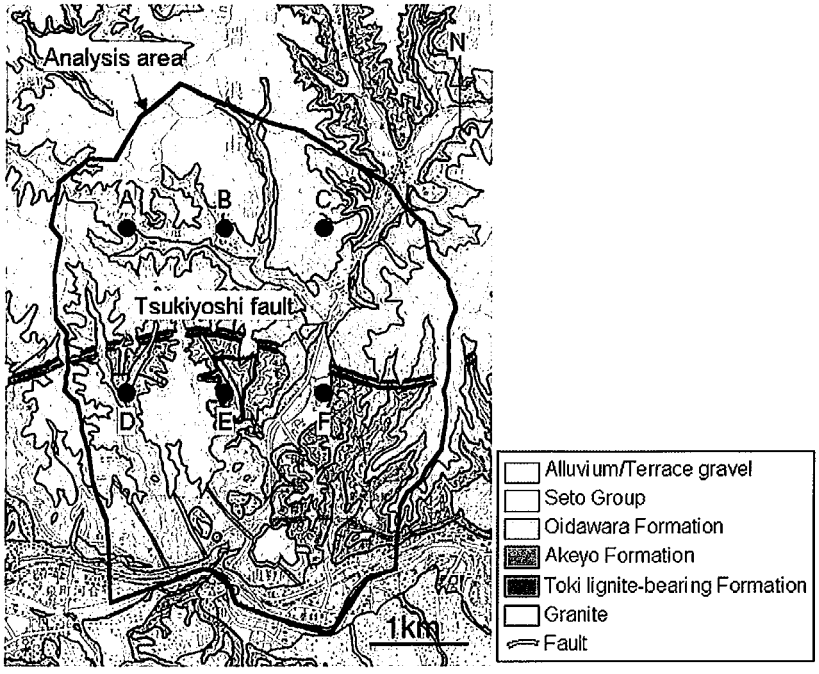

Fig. 3. Geological map of the Tono region.

Table 1
Details of the site investigation

Survey	Method	Content
Literature survey	Topographic map	Topographic condition
	Geological map	Geological condition
Aerial investigation	Landsat imagery	Lineament distribution
	Spot imagery	
	Aerial photos	
Ground investigation	Seismic reflection/refraction profiling	Major discontinuous structure condition
	MT method	Unconformity distribution
	Water balance observation	Precipitation, evapotranspiration, surface water discharge, discharge from the Tono mine (Shobasama site, Garaishi region, Tono mine)
Borehole investigation	Core observation	Geological condition, fracture characteristics
	Borehole TV observation	Fracture depth, strike and dip, fracture aperture, crack sealed vein
	Borehole logging	Caliper logs, formation density logs, groundwater velocity, natural gamma logs, apparent resistivity, micro resistivity, neutron logs, neutron porosity, porosity, RQD, sonic logs, spontaneous potential logs, temperature logs
	Lost circulation measurement	Water way condition (DH boreholes, MIU boreholes) (14 boreholes)
	Hydraulic head observation	Observed in total 158 boreholes including previously existent ones (continuous observation in 48 out of 158 boreholes)
	Hydraulic pressure observation	Pore pressure distribution in vertical direction (total 313 points in 17 boreholes)
	Hydraulic test	Pulse test, slug test, pumping test (292 points in 15 boreholes)

In aerial investigations, the Landsat imagery, spot imagery, and aerial photos were used to identify the distribution of lineaments as shown in Fig. 4 because these observed lineaments substantially follow the distribution of trace length of faults distributed in Japan (Fig. 5; Sawada et al., 2002).

In surface-based investigations, main geological structures such as a formation boundary, unconformity, and the Tsukiyoshi fault have been identified thorough a seismic reflection and refraction profiling. The MT (Magneto-Telluric) method allowed us to identify the spatial distribution of unconformities along the boundary between the Toki granite, which showed high resistivity, and the Neogene sedimentary, which is identified by low resistivity (Fig. 6). The parameters used in water balance calculations such as precipitation, evapotranspiration, river discharge and mine discharge from the Tono mine have been measured.

In addition to the above aerial and surface-based investigations, we also conducted borehole investigations including deep and shallow drilling. The Shobasama site had four boreholes (MIU-1 ~ 4) with depth from 500 m to 1000 m and Fig. 2 illustrates the location of 13 boreholes (DH−1 ~ 13) in the Tono region. The shallow drilling includes 20 boreholes around the Tono mine with depth less than 200 m.

The geological characteristics of the site such as fracture characteristics, distribution of hydraulic conductivities, groundwater table, and pore pressure distributions have been obtained through a series of borehole investigations. The details of the investigation can be found in Table 1.

The water pressure response experiments were performed at deep boreholes as shown in Fig. 7 (Takeuchi et al., 2003). MIU-2 borehole, which is located at the center of the site and had a packer in the Tsukiyoshi fault zone, sent hydraulic signals to the neighboring boreholes by opening and shutting the packer. Upper and lower parts of the Tsukiyoshi fault zone showed their responses at MIU-3 borehole as shown in Fig. 8 and hydraulic response pathways were identified (Fig. 9).

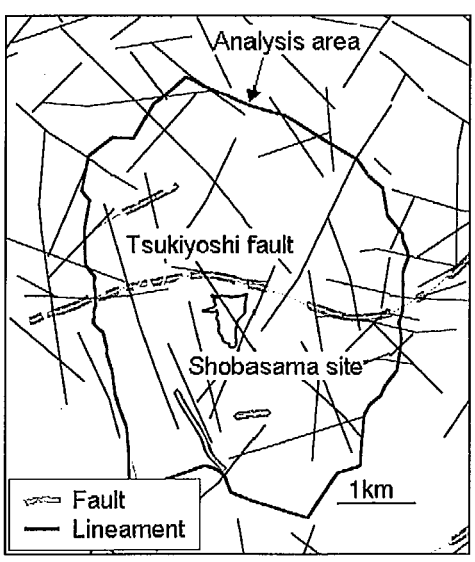

Fig. 4. Lineament distribution in the Tono region.

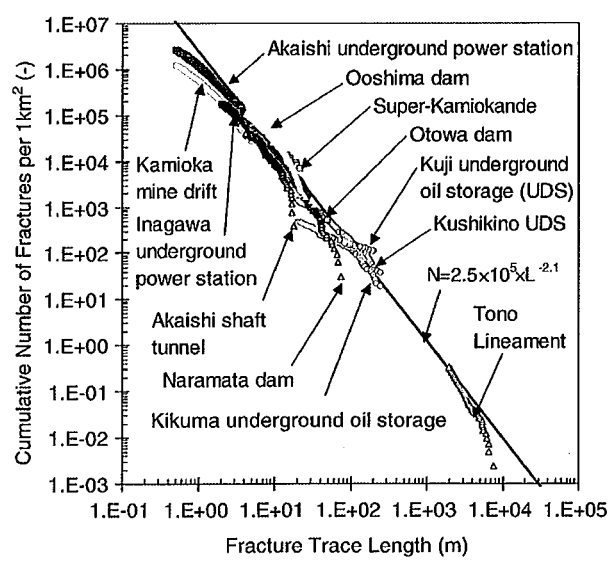

Fig. 5. Distribution of fracture trace length.

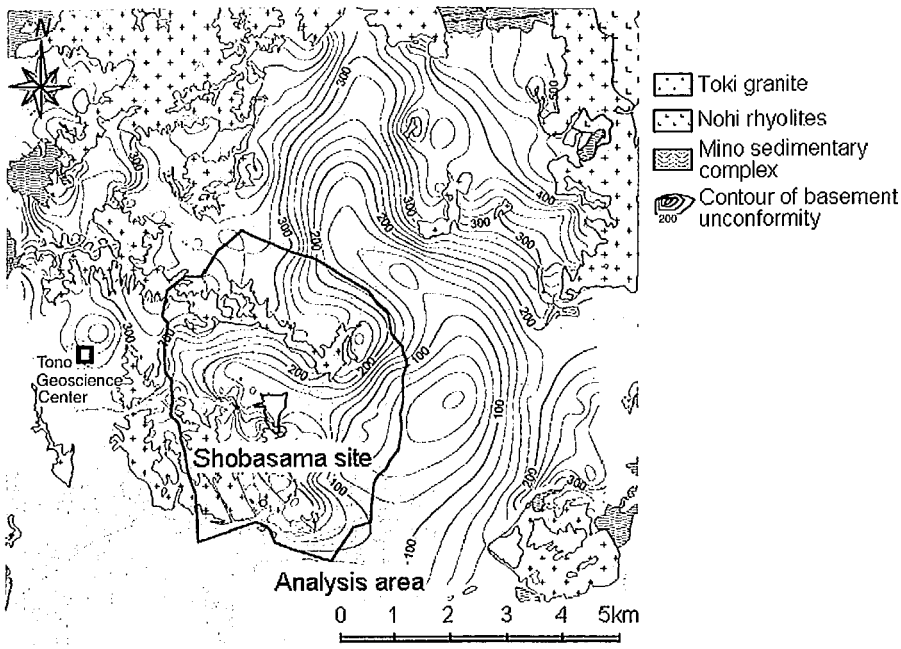

Fig. 6. Altitude distribution of unconformity.

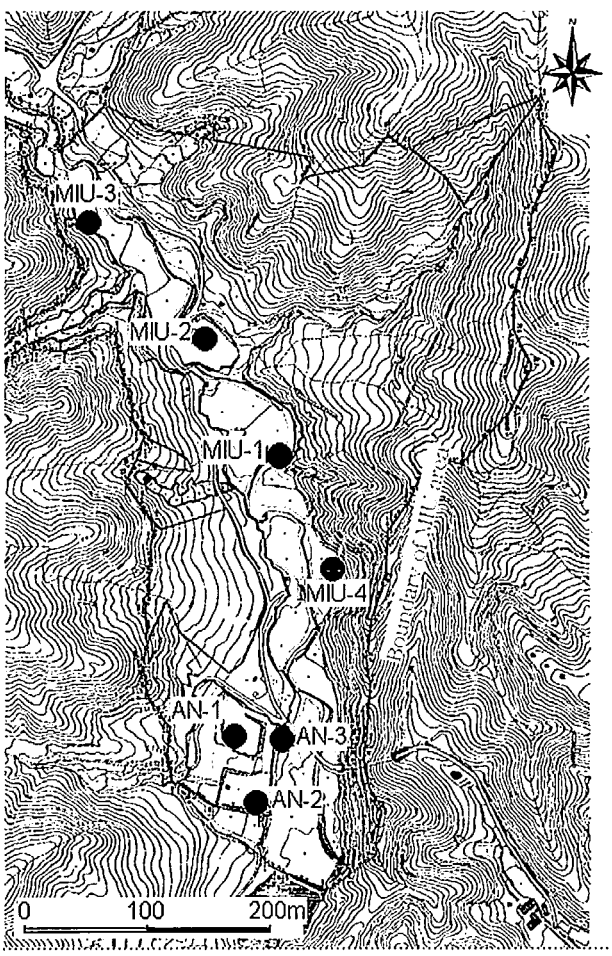

Fig. 7. Boreholes for water pressure response tests.

We also conducted a regional-scale groundwater flow analysis for an area of 30×30 km around the Tono area in order to determine a site-scale assessment area of this study (Saegusa et al., 1998).

3. Analysis conditions

3.1. Assessment area

The assessments were conducted in an area of 6 km×4 km surrounded by ridges and the Toki River as shown by a solid line in Fig. 2, which were considered to be hydrologic boundaries and it was found that the groundwater flow within the area was less affected by the surrounding topography from the results of the previous study (Saegusa et al., 1998). The bottom impermeable boundary was set at altitude of −3000 m taking account of allowance of the depth because the previous study demonstrated that groundwater flow was minimal in the zone deeper than altitude of −2000 m.

3.2. Comparison methods for the results

We evaluate uncertainties by comparing simulation results. We particularly focused on the travel times, shapes, and lengths of flow pathways from four altitude points (−250, −500, −750 and −1000 m) of six stations (A to F stations illustrated in Fig. 3), located in both the northern and southern parts of the Tsukiyoshi fault zone, to the domain boundary, because the travel time and length of flow pathway are necessary for the safety assessment of high-level nuclear waste disposal. It is noted that we used travel time calculated from Darcy velocity in this study because there was no data for estimating effective porosities which are required for calculating the true velocity.

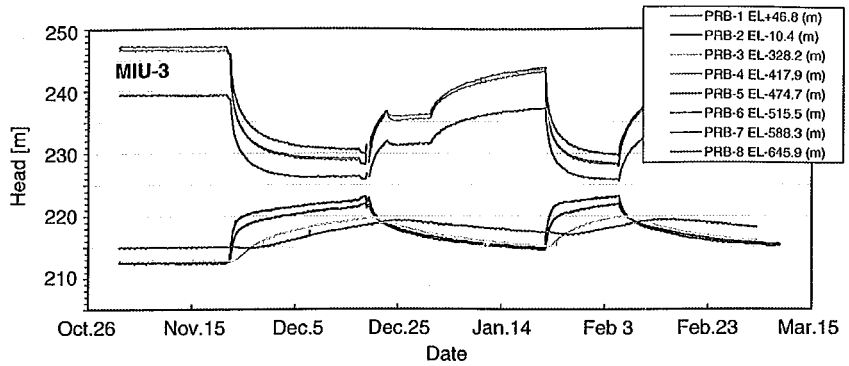

Fig. 8. Results of water pressure response test for MIU-3.

In numerical analyses using TOUGH2 and EQUIV_FLO, which use a stochastic approach to represent porous media, we performed ten realizations to create porous media and conducted groundwater analysis to calculate the travel time and length of flow pathway in each realization. We used the average values and variance of these parameters to compare model cases.

3.3. Analysis conditions

In this study, in order to evaluate uncertainties originating from modeling porous media and fault structures, a series of analyses was performed with a set of conditions, such as domain geometry and size and boundary conditions.

For the upper boundary condition, we assume that it is a constant head boundary condition and the ground water table is located 5 m below the ground surface. This is because the elevation of the ground water table and surface elevation shows a strong linear relationship (Fig. 10) and it is reasonable to assume that the groundwater table mimics the ground surface. Based on a study which included large-scale groundwater flow modeling (Suyama and Saegusa, 2000) we assigned the following lateral boundaries along the domain: a constant hydrostatic pressure boundary was assigned along the ridge and a constant head boundary was set along the Toki River because it was considered to be a discharge area of deep groundwater. A no-flow boundary was assigned to the downstream part of the Toki River. The contribution of the Tono wildcat uranium mine, which is located about 0.7 km away from the Shobasama site in the north-west direction as shown in Fig. 2 and has about 1.3 km drift at the depth of about 130 m, to the regional groundwater flow system was not taken into account in this study because the steady state groundwater flow into the mine was small and was considered to have little impact on groundwater flow. This is because total discharge from the mine, approximately 0.6×10^{-3} m^3/s, is two orders of magnitude smaller than that from the vertical boundary where we estimated the flow to be approximately a 2–30 to $2\text{–}3000\times10^{-3}$ $m^3/s/m^2$.

In order to evaluate a decrease in uncertainties when a new set of data is included, we performed analyses which involve the boundary conditions, which are described in

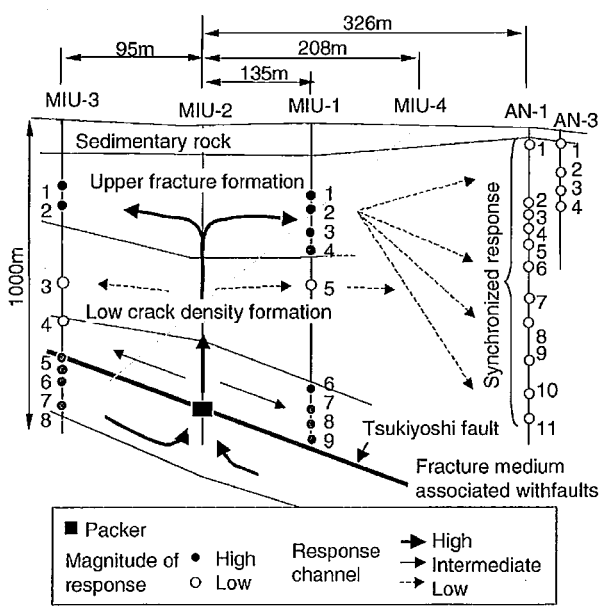

Fig. 9. Water flow channels identified in water pressure response test (Takeuchi et al., 2003).

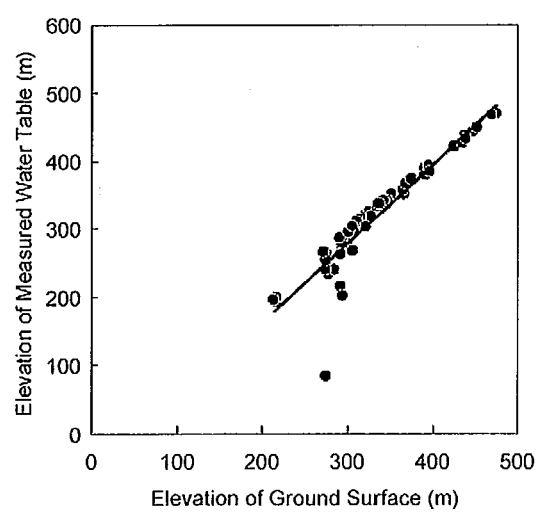

Fig. 10. Relationship between elevations of ground surface and measured water table.

Table 2
Analysis condition

	Setup condition
Analysis area	Top: land surface Lateral: solid line shown in Fig. 2 Bottom: E.L. −3,000 m
Geological structure	Account for sedimentary rocks, granites and the Tsukiyoshi fault (low and high conductivity zones) (lineaments are considered)
Boundary condition	Top: constant heads at G.L.−0.5 m Lateral: constant heads along ridges and the Toki river but no flow at lower portion of the river Bottom: no flow (the Tono mine is not considered)

Table 2, with a new set of observation data from the area of the Tsukiyoshi fault. This data set was obtained from a relatively large area and contains the results from water pressure response experiments (Takeuchi et al., 2003) which are very useful to improve regional-scale groundwater flow analysis. We did not impose any restriction with respect to modeling approaches for the geological structures.

4. Modeling approach

In regional-scale groundwater flow modeling it is very common to use continuous models, which can handle macroscopic heterogeneity of hydraulic conductivity fields, instead of discrete models which focus on microscopic fracture structures because it is difficult to obtain detailed geological information in a regional scale. Hence, we used three continuous models, TOUGH2, EQUIV_FLO, and Don-Chan to investigate the effects of conceptual models on groundwater flow analyses (Table 3). The following sections illustrate the features and approaches towards porous media modeling of each model.

4.1. TOUGH2

TOUGH2 is a numerical code designed to simulate three-dimensional multi-phase flow and transport using an integral finite difference method for space discretization (Pruess, 1991). We used the following simplified governing equation in this study:

$$\mathrm{div}\left[k\frac{k_r}{\mu}\rho\nabla(P+\rho gz)\right]-\frac{\partial}{\partial t}\rho\phi S=0 \quad (1)$$

where, k [m^2] is intrinsic permeability, k_r [−] is relative permeability, P [Pa] is pressure, μ [kg/m s] is viscosity, ρ [kg/m^3] is density, g [m/s^2] is the gravitational acceleration, z [m] is height, ϕ [−] is porosity, S [−] is saturation rate and t [s] is time. The study domain was discretized using 39,400 box elements. The size of these elements is 100 m × 100 m in x- and y-directions, and variable size in z-direction ranging from 50 m to 100 m in such a way that they become finer as the aquifer becomes thinner. A stochastic approach was used to generate the hydraulic conductivity field of the domain which consists of sedimentary rocks and granite. Data sets required for stochastic hydraulic conductivity generation were obtained from in-situ hydraulic conductivity measurements or based on the log-normal distributions illustrated in Fig. 11.

The location of the Tsukiyoshi fault was assigned deterministically as shown in Fig. 12 (a) and the initial hydraulic conductivity value was 1.0×10^{-7} m/s according to the average value of the log-normal distributions (Fig. 11) obtained from literature.

Table 3
Simulation settings for three modeling approaches

	TOUGH2	EQUIV_FLO	Don-Chan
Numerical methods	Integral finite difference method	Finite element method	Finite difference method
Modeling methods of hydrogeologic structures	Generate heterogeneous media based on a stochastic approach assuming log normal distribution of hydraulic conductivity	Generate heterogeneous media by calculating hydraulic conductivity tensors of fractures obtained based on a stochastic approach	Generate channel networks with homogeneous permeable fields which consist of the mean of hydraulic conductivity
Simulated domain	4 km×6 km area surrounded by ridges and the Toki river		
Discretization	Cells: 39,400	Elements: 255,841 Nodes: 45,787	Number of pipes: 1,540,117 Pipe interval: <100 m
Boundary conditions	Top: constant heads at land surface Bottom: no flow at E.L. −3,000 m Lateral: no flow at south along Toki river and constant heads at the rest (Large-scale analysis results obtained from Suyama and Saegusa (2000))	Top: constant heads at 5 m below land surface Bottom: no flow at E.L. −3,000 m The Toki river: constant heads of 0 m	Top: constant heads at 5 m below land surface Bottom: no flow at E.L. −3,000 m Lateral: no flow at south along Toki river and constant heads at the rest (Large-scale analysis results obtained from Suyama and Saegusa (2000))
Modeling structures	Sedimentary rock, unconformity, granite, the Tsukiyoshi fault	Sedimentary rock, unconformity, Granite (including weathered zones and high density fracture media), the Tsukiyoshi fault (including fracture media)	Sedimentary rock, unconformity, granite, the Tsukiyoshi fault, Lineaments
Hydraulic conductivity	Sedimentary rocks: $2\times10^{-9}\sim1\times10^{-7}$ m/s Granite: $5\times10^{-9}\sim1\times10^{-7}$ m/s Fault fracture: 8×10^{-7} m/s Fault clay: 6×10^{-9} m/s	Sedimentary rocks: $1\times10^{-9}\sim1\times10^{-7}$ m/s Granite: 2×10^{-9} m/s(ave.) Fault fracture: 4×10^{-8} m/s(ave.) Fault clay: 1×10^{-10} m/s	Sedimentary rocks: $2\times10^{-8}\sim2\times10^{-6}$ m/s Granite: $3\times10^{-9}\sim2\times10^{-6}$ m/s Fault fracture: 2×10^{-7} m/s Fault clay: 1×10^{-10} m/s

We calibrated the results from the water pressure response experiments at MIU-3 borehole as shown in Fig. 8 and modified the modeling conditions accordingly. In TOUGH2 modeling, we modified the values of hydraulic conductivity for each rock layer, such as the granite layer and the Tsukiyoshi fault zone. The fault zone, which is considered to consist of three zones: lower, middle, and higher permeability zones, are modeled in upper and lower parts of the fault. Hydraulic conductivity for the granite layer and those zones are decreased or increased by a factor of 0.1, 0.1, 45, and 3, respectively.

Please refer Doughty and Karasaki (2001) for a detailed discussion of porous media modeling approach.

4.2. EQUIV_FLO

EQUIV_FLO (Shimo et al., 2001) uses a finite element method to simulate three-dimensional saturated and unsaturated flow. The governing equation used in the code is:

$$k_r(\theta)k_{ij}\nabla^2(h)-\left(C+\frac{\theta}{n}S_s\right)\frac{\partial h}{\partial t}=0 \qquad (2)$$

where k_r [−] is relative hydraulic conductivity, θ [−] is water content, k_{ij} [m/s] is saturated hydraulic conductivity tensor, h [m] is hydraulic head, C [1/m^3] is specific water capacity, n [−] is porosity, and S_s [1/m] is specific storage.

We divided the granite formation into three groups according to the fracture density which are the ordinary-fractured zone, the highly-fractured zones including lower parts of unconformities and along the Tsukiyoshi fault, and applied a cluster analysis to these groups in order to obtain distinguishable fracture groups as shown in Fig. 13. Each group was characterized using several parameters as shown in Table 4. Based on these parameters, we stochastically generated fracture networks to represent the domain. We assigned the value of three-dimensional fracture density in the model in such a way that the value of its one-dimensional density coincided with that of borehole observation at the

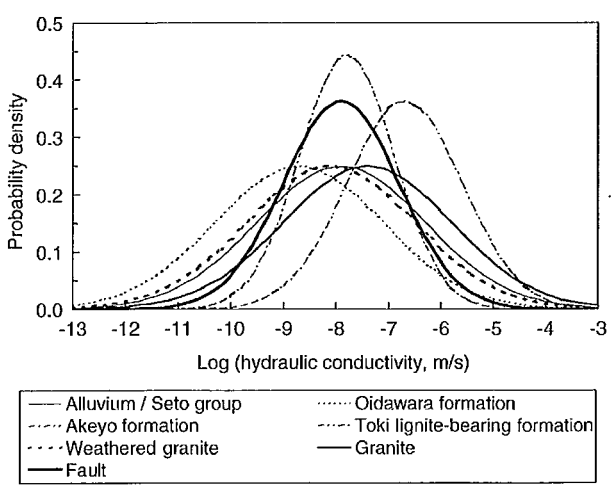

Fig. 11. Probability density functions for hydraulic conductivities used for modeling.

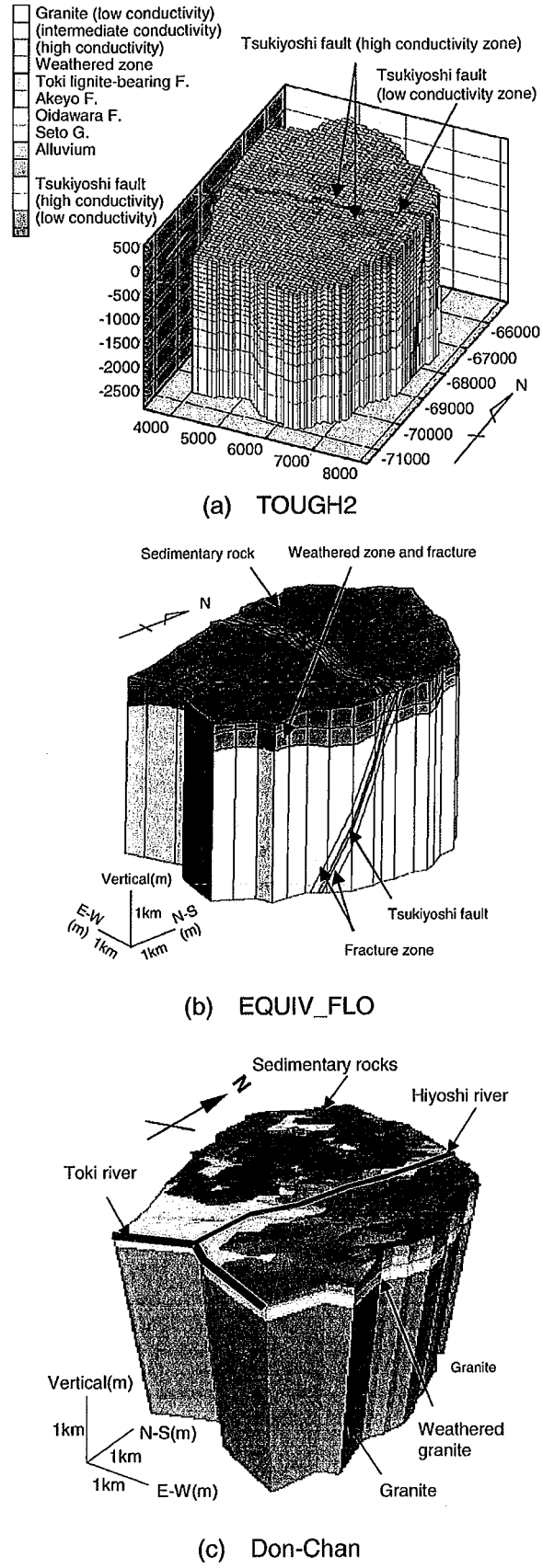

Fig. 12. Bird's eye view of analysis model.

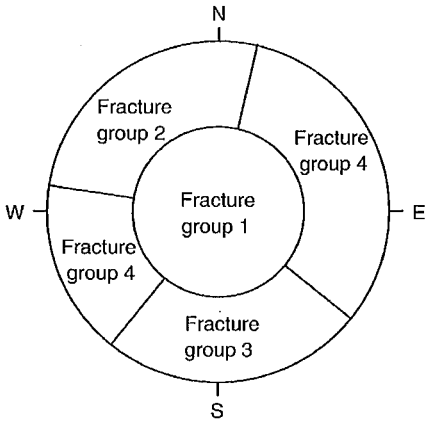

Fig. 13. Four fracture groups in highly-fractured media of the Toki granite obtained through cluster analysis.

site. Directional distribution ($f(\phi, \theta)$), radius distribution($f(r)$), and aperture distribution ($f(d)$) were assumed to follow Bingham, power law, and negative exponential distributions respectively, and can be expressed as:

$$f(\phi, \theta) = c \cdot \exp\{(\kappa_1 \cos^2\theta + \kappa_2 \sin^2\theta) \cdot \sin^2\phi\} \tag{3}$$

$$f(r) = \frac{b-1}{r_{\min}} \left(\frac{r_{\min}}{r}\right)^b, \; r \geq r_{\min} \tag{4}$$

$$f(d) = \rho(d_0) \cdot \exp(-\lambda d) \tag{5}$$

where, θ [°] is the angle from z-axis, c is a constant, κ_1, κ_2 [−] are partition coefficients, b [−] is an exponential constant, r [m] is fracture radius, $r_{\min}$ [m] is minimum radius, d [m] is hydraulic fracture aperture, $\rho_d(0)$ [1/m] is cumulative 1-D fracture frequency at $d=0$, and $1/\lambda$ [m] is average fracture aperture.

Numerical hydraulic conductivity measurements were conducted in the stochastically generated domain and we modified an exponential constant (b) and average fracture aperture ($1/\lambda$) in the above equations in order to match hydraulic conductivity distributions obtained from the site.

We discretized the domain containing discrete fracture networks with finite element method and calculated the hydraulic conductivity tensor shown in Eq. (6) using the crack tensor theory based on the fractures in each mesh. Heterogeneous continuous porous media equivalent to the discrete fracture network was generated based on the hydraulic conductivity tensor of the fracture network.

$$k_{ij} = k_{ij}^m + \frac{g}{12\nu\Delta V} \sum_l \Delta A_l^c t_l^3 (\delta_{ij} - n_i n_j) \tag{6}$$

$$S = S^m + \frac{1}{\Delta V} \sum_l \Delta A_l^c d_l S_l^c \tag{7}$$

where, k_{ij}^m [m/s] is hydraulic conductivity tensor of porous medium, g [m/s^2] is the gravitational acceleration, ν [m^2/s] is the coefficient of kinematic viscosity, ΔV [m^3] is element volume, ΔA_l^c [m^2] is an area of fracture l in an element volume ΔV, δ_{ij} [−] is Kronecker delta, n_i [−] is direction cosine of normal vector of fracture l, and S^m [1/m] is specific storage of porous media.

A deterministic approach was used to model the Tsukiyoshi fault zone by using information about the location as shown in Fig. 12 (b), width, and hydraulic conductivity of the fracture zone obtained from the site.

We calibrated the results from the water pressure response experiments (Fig. 8) and modified the values of hydraulic conductivity for each rock layer in a manner which is the same as in TOUGH2 modeling. Hydraulic conductivity for lower and upper higher permeable zones of the Tsukiyoshi fault zone are increased by a factor of 10 and 100, respectively. We assume that the fault includes a high permeable fracture and assigned a value equal to 1×10^{-4} m^2/s.

See Shimo et al. (2001) for more details of this media modeling approach.

4.3. Don-Chan

Don-Chan code simulates three-dimensional groundwater flow using a finite difference method. The governing equation can be described as:

$$k_{ij} \nabla^2(h) - S_s \frac{\partial h}{\partial t} = 0 \tag{9}$$

Please note that all parameters used in Eq. (9) are already defined in equations used in TOUGH2 and EQUIV_FLO.

This code is designed to represent fracture networks as a step structure made of the combinations of main and branch fractures (Fig. 14). The code focuses on water pathways developed on fracture intersections and planes, which forms a step structure, and fracture edges. These water pathways are deterministically assigned as a pipe network as illustrated in Fig. 15. In other words, fracture networks in granite are modeled as lattice-shaped equally-spaced pipe networks and the sizes of cross-sectional area are determined in such a way that hydraulic conductivity over unit volume is equal to hydraulic conductivity measured at the site.

The location of the fault and lineaments are deterministically modeled based on in-situ data. We calibrated pore water pressure distribution data and obtained hydraulic conductivities of pipes assigned parallel and perpendicular to the fault zone. Based on this anisotropic hydraulic conductivity distribution, a low hydraulic conductivity zone located in the middle of the fault and high permeable fractures located at the edges were modeled.

In the calibration process, the results from the water pressure response experiments (Fig. 8) was used again, and

Table 4
Characteristics of fractures

	Setup condition
Direction	Bingham's distribution (3 rock types×4 groups)
Radius distribution	Power-law distribution Power 3, $r_{\min}$=70 m, $r_{\max}$=3,000 m
Density	1-D density: 0.0679 fracture/m (about 15 m per fracture) 3-D density: about 5.87×10^{-7} m^2/m^3
Fracture aperture	Hydraulics: Negative exponential distribution Solute transport: empirical law $2\sqrt{T}$

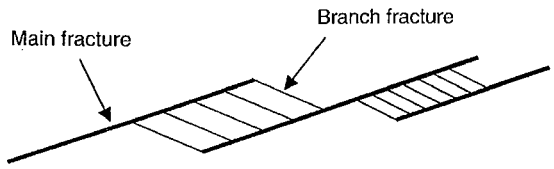

Fig. 14. Step structure of fracture networks.

we model the sedimentary rock and weathered granite rock layers in detail as illustrated in Fig. 12 (c). All rock layers except the non-weathered granite layer are assumed to have an anisotropic hydraulic conductivity, in which vertical hydraulic conductivity is two to three order magnitudes smaller than horizontal hydraulic conductivity, based on the results from the calibration process. We model faults along the lineament (Fig. 16) and assign anisotropic feature of hydraulic conductivity, in which hydraulic conductivity perpendicular to the faults is two to four order magnitude smaller than hydraulic conductivity parallel to the faults. Please note that we did not find that any of the models is superior to the other during the calibration processes.

Please refer to Morita and Watanabe (2001) for a detailed discussion of porous media modeling approach.

In summary, TOUGH2 and EQUIV_FLO mainly focus on modeling of porous media heterogeneity in space, and Don-Chan is designed to model anisotropy of porous media. As described the above, all three models simulate the computational domains in which higher and lower hydraulic conductivity are assigned for the both sides of the fault zone and perpendicular to the fault zone, respectively. This new assignment highlights a difference between two zones.

5. Result

As noted in Table 3, TOUGH2 and EQUIV_FLO did not model the faults other than the Tsukiyoshi fault, whereas Don-Chan modeled not only the Tsukiyoshi but also the lineaments in the domain. TOUGH2 and Don-Chan used the hydraulic conductivity distribution obtained from in-situ hydraulic tests, whereas EQUIV_FLO used fracture properties for assigning hydraulic conductivities of hydrogeological structures. These differences among three models yield the differences among their results.

Figs. 17 and 18 illustrate mean, maximum, and minimum of pathway length and travel times, respectively, which are

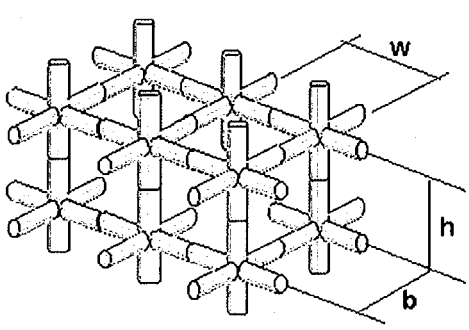

Fig. 15. Fracture network structure represented by a lattice of a pipe network.

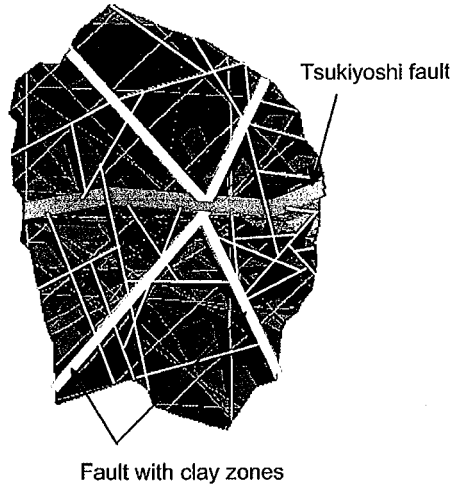

Fig. 16. Plan view of faults in Don-Chan model.

calculated based on ten realizations conducted in TOUGH2 and EQUIV_FLO simulations. The black marker and upper–lower bar show the mean and maximum–minimum value of each realization, respectively. It can be seen from the figure that the variance among realizations is greater in TOUGH2 than that of EQUIV_FLO. It also can be seen from the results of TOUGH2 analyses that the maximum value of travel length is about seven times larger than the minimum value and that the maximum value of travel time is more than three orders of magnitude larger than the minimum value in some locations.

Fig. 19 illustrates the horizontal projection view of migration pathways obtained from the three models. Please note that only the results of one realization are shown for TOUGH2 and EQUIV_FLO. As shown in Fig. 19, although all three models show that bulk groundwater flow direction is from north to south according to the topography, differences between pathways can be found which are caused by differences in geological modeling. In TOUGH2 results, groundwater flow tends to flow upward along the fault in the northern side of the fault and at the point F in the southern side of the fault, because the high permeable fracture zones along the Tsukiyoshi fault are modeled.

Similarly, the EQUIV_FLO results show upward groundwater flow in the north side of the fault toward the ground surface along the fault because the model takes account for both a low permeability zone at the center of the Tsukiyoshi fault and the highly permeable fracture zone along both sides of the fault. On the other hand, groundwater flows toward the east direction along the fault in the southern side of the fault. The pathway lengths in the northern side of the Tsukiyoshi fault tend to be longer than those in the southern part of the fault, and the pathway lengths in the western side of the region tend to be longer than those in the eastern side in the results of TOUGH2 and EQUIV_FLO as shown in Fig. 20.

In Don-Chan, migration pathways are significantly different from those calculated in TOUGH2 and EQUIV_FLO because we model faults along the lineaments which have anisotropic hydraulic conductivities. We can no longer observe groundwater flow toward the Toki River in the south side of the

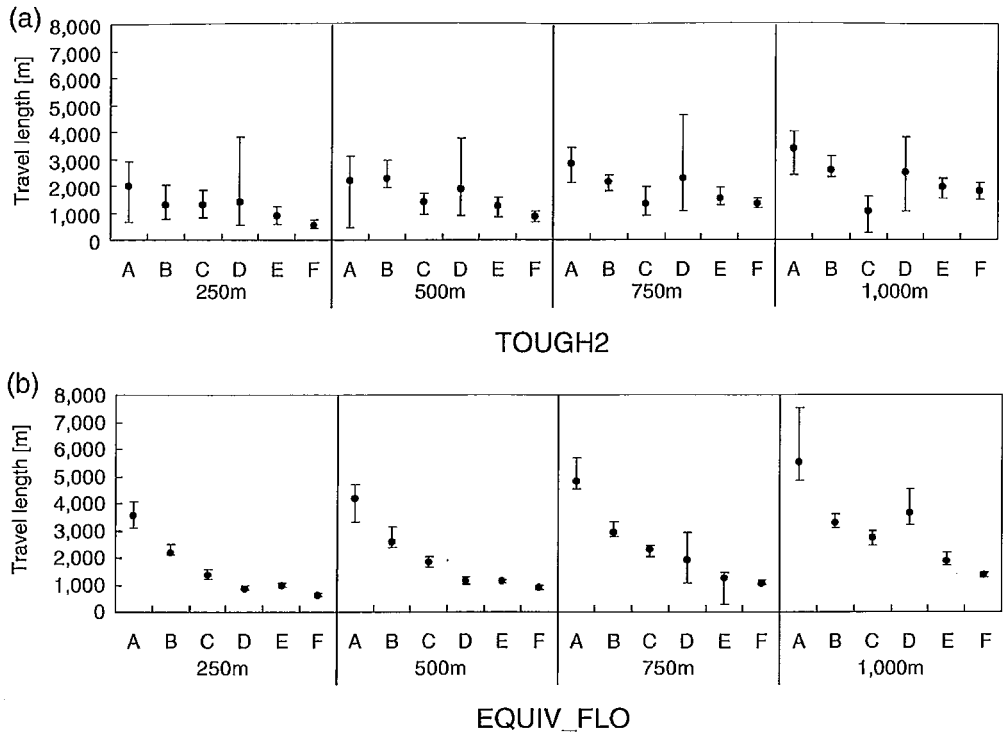

Fig. 17. Variance of travel distance among realizations.

Tsukiyoshi fault. The results from Don-Chan model simulations showed that the lineaments greatly affected the groundwater flow system; there are uncertainties originating from modeling of lineaments due to a lack of site observations indicating whether faults exist along the lineaments. Modeling of the lineaments depends on the modeler's expertise. In

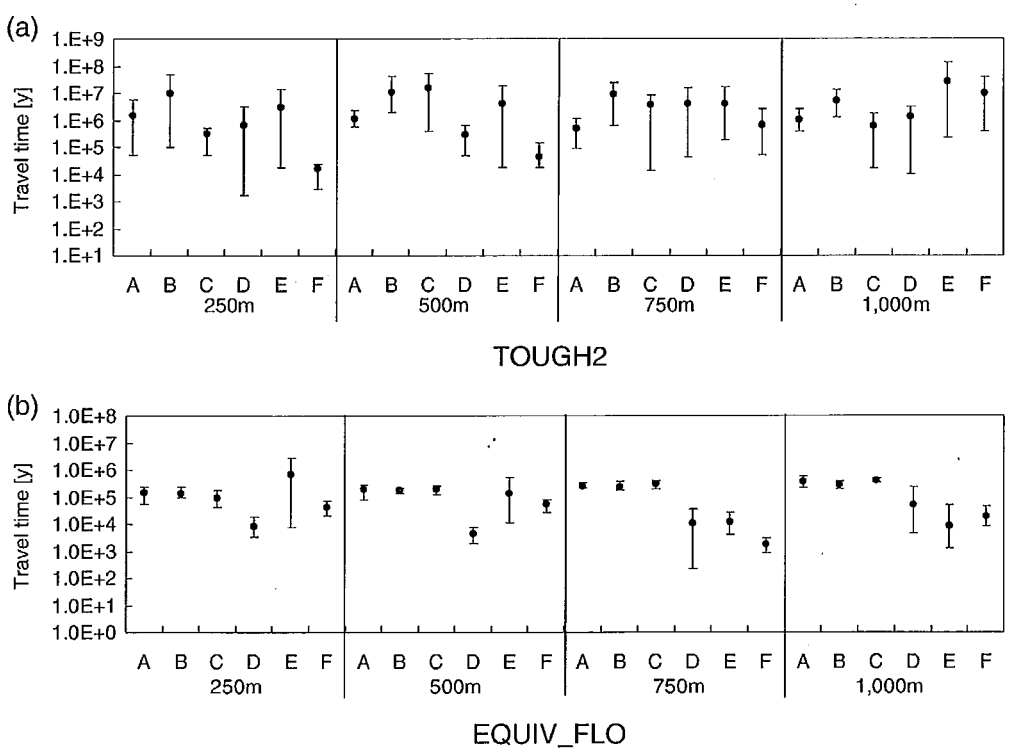

Fig. 18. Variance of travel time among realization.

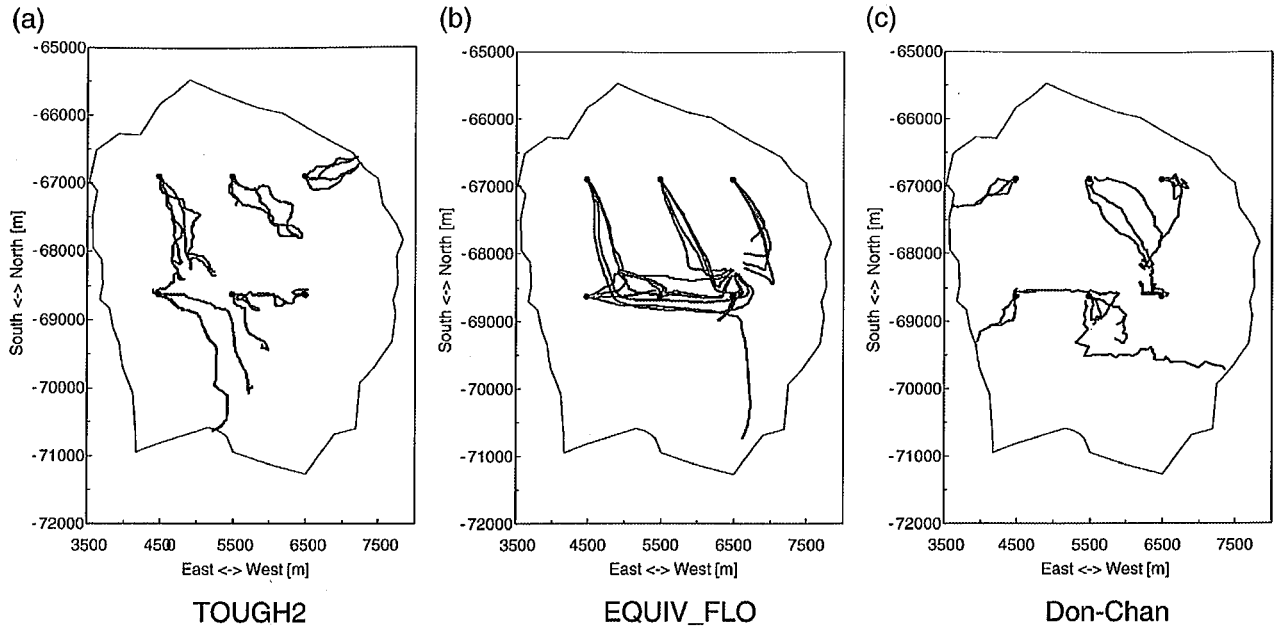

Fig. 19. Planar projection of migration paths.

order to reduce this type of uncertainties site investigation to characterize the lineaments is required.

The maximum difference of travel time among the three modeling approaches is three orders magnitudes, whereas the maximum difference of pathway lengths is only 2.5 orders of magnitude at point E at 1,000 m depth as shown in Fig. 21. TOUGH2 tends to yield longer travel times than the others. Although the pathway lengths from point E of 1,000 m depth in TOUGH2 and EQUIV_FLO are almost the same, TOUGH2 yields three orders magnitude longer travel time than EQUIV_FLO.

As can been seen in the simulation results, uncertainties among the three models decrease because the hydraulic condition near the Tsukiyoshi fault, which is one of uncertainty factors and greatly affects the overall groundwater system, was modeled in detail with in-site hydraulic response measurements. Geological structures modeled in detail using site measurements change among the models. For example, EQUIV_FLO modeled high permeable fractures zone between overburden sedimental rock formation and basement rock formation based on borehole investigation and Don-Chan modeled faults along the lineament observed by aerial investigations. Because the models focus on different geological structures which could affect overall groundwater flow uncertainties cannot be always decreased in the same manner. In order to reduce uncertainties, it is critical to identify the role of geological structures, such as highly permeable fractures and faults along the lineaments, through field investigations.

6. Conclusion

Sources of uncertainties and their impacts in regional-scale groundwater flow analyses were investigated in this study. We found that uncertainties originating from modeling approaches, which include modeling geological structures such as fault and assigning heterogeneity for porous media, have a quite large impact on regional groundwater flow. Especially, quite large low- and high-permeable structures such as faults and fracture zones that define migration pathway have a greater impact on a regional groundwater flow than methodology of assigning heterogeneity for porous media. The modeling approach including what kind of geological structure is to be modeled and how heterogeneous

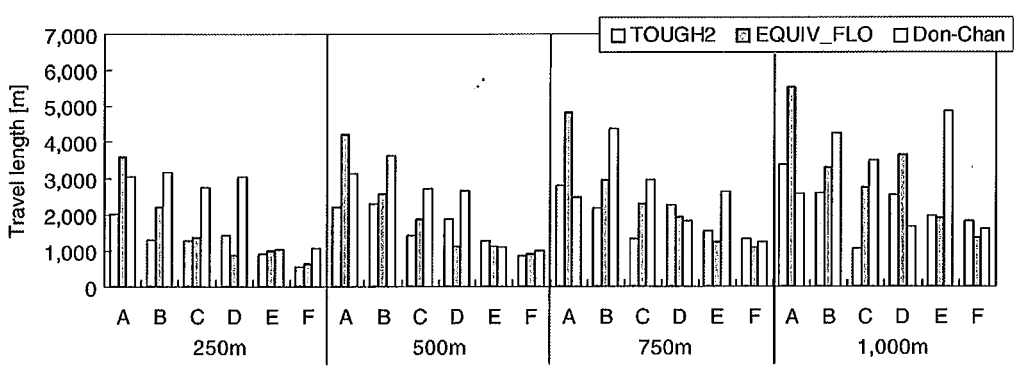

Fig. 20. Distribution of travel distance.

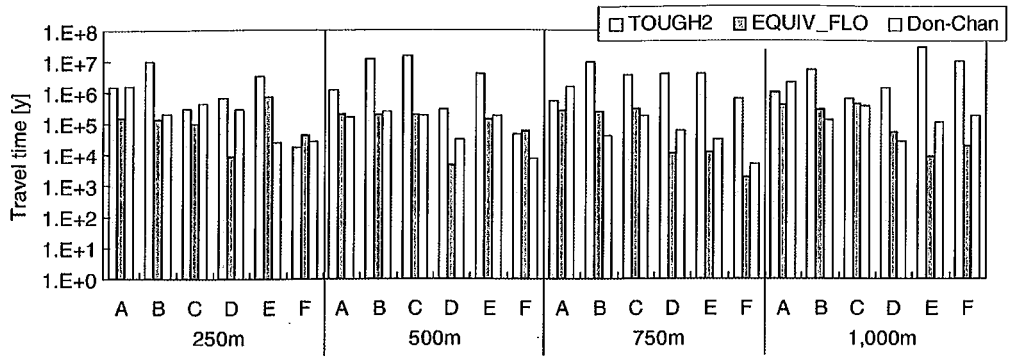

Fig. 21. Distribution of travel time calculated using Darcy's velocity

properties are to be assigned when we solve a regional groundwater flow is highly dependent on the modeler's idea even when the same dataset and information are provided. Therefore, it can be concluded that the modeler's concept has more effect on groundwater analyses compared to modeling approaches itself with respect to increasing uncertainties. Because hydrological and geological data sets which can be obtained from the site are limited, interpretations of such data sets, which require computational setup for groundwater analyses, greatly depend on the ideas and concepts of modelers. Different interpretations among the modelers lead to different computational setups, such as analysis domain, boundary conditions, and porous media, and these results in significant differences in analysis results.

In order to reduce uncertainties originating from the ideas and concepts of modelers, it is critical to obtain effective and necessary site data.

Uncertainties originating from the ideas and concepts of modelers can be effectively reduced by making constraint conditions, such as boundary conditions and hydrological structures to be modeled. In order to achieve this, it is necessary to eliminate errors in interpretations among the modelers and they should share common standards regarding boundary conditions and analysis domain in order to reduce uncertainties. One way of solving this problem is as demonstrated in the previous studies(Zimmerman et al., 1998), modeling approaches and analyses improve as the amount of labor and time spent increase, i.e., modelers' understanding of the system improves and the way they interpret the system changes. In order to enhance our understanding of regional-scale groundwater flow systems, we should facilitate discussion between modelers and site investigators, who tend to work independently, and keep devoting all necessary resources to achieve this.

Another way of reducing uncertainties is by incorporating data from site hydraulic response measurements that could reduce uncertainties originating from modeling of hydrogeological structures. However, uncertainties were only slightly reduced by incorporating site data in this study because modelers focus attention on different aspects of the model calibration processes. As illustrated in Fig. 22, we need an iteration process between site investigation and computational analysis. This process includes identification of uncertainty factors through incorporation of site data to computational analyses, and site investigation driven by analyses' results to specify such uncertainty factors.

Uncertainties originating from modeling approaches decrease as the amount of labor and time spent increase, and iterations between investigation and analyses increases as it can be seen in Fig. 23. Uncertainties in the early stage will greatly decrease as amount of information from the site and labor and time spent increase. In the final stage, porous media heterogeneity is the main factor which causes uncertainties. In a future study, we are going to (1) develop an efficient

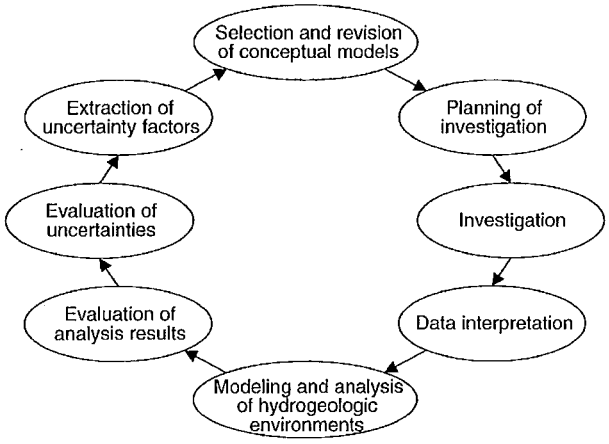

Fig. 22. Flowchart of investigation and evaluation.

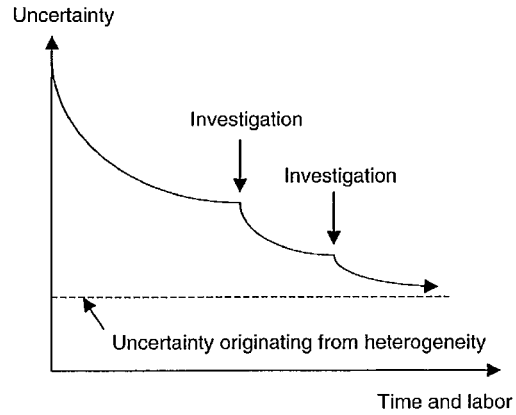

Fig. 23. Relationship between magnitude of uncertainty and labor and time spent by modelers.

investigation method and steps for each uncertainty factors, (2) improve the accuracy of data interpretation, and (3) develop an efficient method to decrease uncertainties originating from modeling approaches.

Acknowledgments

Mr. Shinji Takeuchi of the Tono Geoscience Center, Japan Atomic Energy Agency and Mr. Hideaki Osawa and others provided site data for this study and the authors greatly appreciate their support. We thank Mr. Katsushi Nakano and Mr. Keiichiro Wakasugi of Japan Atomic Energy Agency for their comments and suggestions on an earlier draft of this manuscript. The support of Mr. Nozomu Nishijima of Taisei Corporation and Mr. Yutaka Morita for modeling analyses and Mr. Kenichi Hosono of Geoscience Research Laboratory for organizing the analysis results is greatly appreciated. The authors are also grateful to Dr. Motomu Ibaraki of the Ohio State University for a review of the manuscript.

References

Doughty, C., Karasaki, K., 2001. Evaluation of uncertainties due to hydro-geological modeling and groundwater flow analysis (2) -LBNL effective continuum model using TOUGH2-. Symposium on groundwater flow problems in fractured rock. JGS, pp. 259-268.

Foglia, L., Mehl, S.W., Hill, M.C., Perona, P., Burlando, P., 2007. Alternative ground water models using cross validation and other methods. Ground Water 45 (5), 627-641.

Ijiri, Y., Hata, A., Hosono, K., Sawada, A., 2004. Study on uncertainties of radionuclide migration parameter values obtained from in-situ tracer tests. Journal of JSCE 778/III-69, 85-97.

Ijiri, Y., Saegusa, H., Sawada, A., Nakano, K., Ono, M., 2007. Uncertainty due to conceptual models in a regional scale groundwater flow. Japanese Association of Groundwater Hydrology 67-76.

Japan Nuclear Cycle Development Institute, 1999. H12: Project to establish the scientific and technical basis for HLW disposal in Japan, Second progress report on research and development for the geological disposal of HLW in Japan, JNC TN1400 99-023.

Morita, Y., Watanabe, K., 2001. Effect of hydro-geological conceptual modeling on deep groundwater flow (part 4)-Fracture network analysis for evaluating the groundwater flow and transport affected by large faults-. Symposium on groundwater flow problems in fractured rock. JGS, pp. 279-288.

Nuclear Energy Agency, 1991. Review of safety assessment methods. OECD, Paris.

Pruess, K., 1991. TOUGH2 — A general-purpose numerical simulator for multiphase fluid and heat flow, LBL-29400, UC-251.

Refsgaarda, J.C., van der Sluijsb, J.P., Brownc, J., van der Keura, P., 2006. A framework for dealing with uncertainty due to model structure error. Advances in Water Resources 29, 1586-1597.

Saegusa, H., Inaba, H., Koide, K., Ogata, N., 1998. Simulation of regional scale groundwater flow in Tono area, PNC TN7410 98-004.

Sawada, A., Ohnishi, Y., Ohtsu, H., Ijiri, Y., Nishiyama, S., 2002. Applicability of the concept of fractal to fracture network model in rock mass, ed by Choy, Ryu, Jeon and Moon. Rock engineering problems and approaches in under ground construction, vol.1, pp. 203-210. ISBN 89-53134-0-4 94530.

Selroos, J., Walker, D.D., Ström, A., Gylling, B., Follon, S., 2002. Comparison of alternative modeling approaches for ground water flow in "fractured rock. Journal of Hydrology 257, 174-188.

Shimo, M., Nishijima, N., Fumimura, K., 2001. Evaluation of uncertainties due to hydrogeological modeling and groundwater flow analysis (3)-Taisei equivalent heterogeneous continuum model using EQUIV_FLO-. Symposium on groundwater flow problems in fractured rock. JGS, pp. 269-278.

Suyama, Y., Saegusa, H., 2000. Geological modeling and groundwater flow simulation in the regional hydrogeological study project, JNC TN7400 2000-012.

Takeuchi, S., Shimo, M., Yamamoto, H., Fumimura, K., 2003. Long-term pumping test conducted in 1,000 m length borehole. 32nd Symposium on rock mechanics, JSCE, pp. 173-178.

Wakasugi, K., Webb, E., Makino, H., Ishihara, Y., Ijiri, Y., Sawada, A., Baba, T., Ishiguro, K., Umeki, H., 2000. A Trial of probabilistic simulation for reference case in the second progress report on research and development for the geological disposal of HLW in Japan. PSAM5, vol.4, pp. 1469-1475.

Ye, M., Pohlmannb, K.F., Chapmanb, J.B., 2008a. Expert elicitation of recharge model probabilities for the Death Valley regional flow system. Journal of Hydrology 354 (1-4), 102-115.

Ye, M., Meyer, P.D., Neuman, S.P., 2008b. On model selection criteria in multimodel analysis. Water Resources Research 44, W03428. doi:10.1029/2008WR006803.

Zimmerman, D.A., de Marsily, G., Gotway, C.A., Marietta, G.M., Axness, C.L., Beauheim, R.L., Bras, R.L., Carrera, J., Dagan, G., Davies, P.B., Gallegos, D.P., Galli, A., Gómez-Hernández, J., Grindrod, P., Gutjahr, A.L., Kitanidis, P.K., Lavenue, A.M., McLaughlin, D., Neuman, S.P., RamaRao, B.S., Ravenne, C., Rubin, Y., 1998. A comparison of seven geostatistically based inverse approaches to estimate transmissivities for modeling advective transport by groundwater flow. Water Resources Research 34 (6), 1373-1413.

This work was supported by the U.S. Department of Energy under Contract No. DE-AC02-05CH11231.

DISCLAIMER

This document was prepared as an account of work sponsored by the United States Government. While this document is believed to contain correct information, neither the United States Government nor any agency thereof, nor the Regents of the University of California, nor any of their employees, makes any warranty, express or implied, or assumes any legal responsibility for the accuracy, completeness, or usefulness of any information, apparatus, product, or process disclosed, or represents that its use would not infringe privately owned rights. Reference herein to any specific commercial product, process, or service by its trade name, trademark, manufacturer, or otherwise, does not necessarily constitute or imply its endorsement, recommendation, or favoring by the United States Government or any agency thereof, or the Regents of the University of California. The views and opinions of authors expressed herein do not necessarily state or reflect those of the United States Government or any agency thereof or the Regents of the University of California.